Synthesis, X-ray crystallography, spectroscopy, electrochemistry, thermal and kinetic study of uranyl Schiff base complexes

Zahra Asadi[a], Fatemeh Golzard[a], Vaclav Eigner[bc] & Michal Dusek[b]

[a] Department of Chemistry, College of Science, Shiraz University,
Shiraz, Islamic Republic of Iran

[b] Department of Solid State Chemistry, Institute of Chemical
Technology, Prague, Czech Republic

[c] Institute of Physics AS CR, v.v.i., Prague, Czech Republic
Accepted author version posted online: 01 Oct 2013.Published
online: 30 Oct 2013.

PLEASE SCROLL DOWN FOR ARTICLE

Taylor & Francis
Taylor & Francis Group

Synthesis, X-ray crystallography, spectroscopy, electrochemistry, thermal and kinetic study of uranyl Schiff base complexes

ZAHRA ASADI*†, FATEMEH GOLZARD†, VACLAV EIGNER‡§ and
MICHAL DUSEK‡

†Department of Chemistry, College of Science, Shiraz University, Shiraz, Islamic Republic of Iran
‡Department of Solid State Chemistry, Institute of Chemical Technology, Prague, Czech Republic
§Institute of Physics AS CR, v.v.i., Prague, Czech Republic

Uranyl(VI) complexes [UO_2(L)(solvent)], where L denotes an asymmetric N_2O_2 Schiff base (salpyr, 3-MeOsalpyr, 4-MeOsalpyr, 5-MeOsalpyr, 5-Clsalpyr or 5-Brsalpyr; salpyr is N,N′-bis(salicyliden)-2,3-diaminopyridine), were synthesized and characterized in solution (UV–vis, ^{1}H NMR, cyclic voltammetry) and in the solid-state (X-ray crystallography, IR, TGA, C H N.). X-ray crystallography of UO_2(3-MeOsalpyr) revealed coordination of the uranyl by the tetradentate Schiff base and one disordered solvent, resulting in seven-coordinate uranium. Another disordered solvent was not coordinated. Cyclic voltammetry of [$U^{VI}O_2$(L)(solvent)] in acetonitrile was used to investigate the effect of the substituents of the Schiff base ligands on oxidation and reduction potential. The quasi-reversible redox reaction without any successive reactions was accelerated by groups with lesser electron withdrawing. We also investigated the kinetics and mechanism of the exchange reaction of the coordinated solvent with tributylphosphine using spectrophotometric method. The second-order rate constants at four temperatures and activation parameters showed an associative mechanism for all corresponding complexes with the following trend: UO_2(5-Clsalpyr) > UO_2(5-Brsalpyr) > UO_2(3-MeOsalpyr) > UO_2(4-MeOsalpyr) > UO_2(salpyr) > UO_2(5-MeOsalpyr). It was concluded that the steric and electronic properties of the complexes were important for the reaction rate.

Keywords: X-ray crystallography; Uranyl Schiff base complex; Kinetics of thermal decomposition; Cyclic voltammetry; Kinetics and mechanism

1. Introduction

The majority of high oxidation state complexes of the actinides contain actinyl ions [AnO_2]$^{n+}$, where An = U, Np, Pu; *n* = 1 or 2. In contrast to transition metal dioxo complexes which almost always adopt bent geometries, the actinyl ions are essentially linear [1]. Uranium is the most widely studied actinide because of its occurrence in nature. The chemistry of uranium is dominated by the dioxo or uranyl dication, [UO_2]$^{2+}$, which is found both in aqueous solutions and in the solid state. It is the most thermodynamically stable form of uranium, in contrast to the pentavalent uranyl cation [UO_2]$^+$, which disproportionates in aqueous environment into tetravalent uranium species and [UO_2]$^{2+}$ [2]. Coordination

*Corresponding author. Emails: zasadi@shirazu.ac.ir; zasadi@susc.ac.ir

compounds of uranyl have interesting reactivity, coordination properties, and applications [1–9].

Solvents containing oxygen can coordinate to uranyl with tetradentate Schiff base ligands [10]. The usual coordination number in the equatorial plane of U(VI) is five or six. A penta- or hexa-dentate planar ligand may not have solvent in the equatorial plane [5].

Our group studied the kinetics and mechanism of the addition reaction of tetraaza Schiff base complexes of first-row transition metals with different donors [11–14].

In this paper, our interest is focused on complexes of uranyl with salpyr, 3-MeOsalpyr, 4-MeOsalpyr, 5-MeOsalpyr, 5-Clsalpyr, and 5-Brsalpyr and the solvent MeOH. X-ray crystallography and TG reveal that one methanol coordinates weakly to the uranium center. Thus we can study the kinetics of exchange of this solvent molecule with tributylphosphine and parameters affecting the rate constants of the exchange reaction, such as electronic and steric effects. The effect of substituents on the redox potential of these complexes was studied.

2. Experimental

2.1. *Materials*

Salicylaldehyde, 3-methoxysalicylaldehyde, 4-methoxysalicylaldehyde, 5-methoxysalicylaldehyde, 5-chlorosalicylaldehyde, 5-bromosalicylaldehyde, 2,3-diaminopyridine, uranylacetatedihydrate, methanol, acetonitrile, and potassium bromide for IR spectroscopy, tetrabutylammoniumperchlorate (TBAP), tributylphosphine, $CDCl_3$, and DMSO-d_6 were obtained from Merck, Fluka, Aldrich, and Acros and used without purification.

2.2. *Instruments*

Scanning UV-vis spectra were recorded on a Perkin Elmer Lambda 2 spectrophotometer. ^{1}H NMR spectra were recorded on a Bruker Avance DPX 250 MHZ. IR spectra were recorded on a Shimadzu FTIR 8300 infrared spectrophotometer. Elemental microanalyses were performed with a CHN Thermo Finnigan Flash EA1112 instrument. Melting points were determined on a BUCHI 535. Thermogravimetric analyzes were recorded with a Perkin-Elmer Pyris Diamond model. Electrochemistry was carried out using Auto lab 302 N. X-ray crystallography was performed by the four-cycle diffractometer Gemini of Agilent Technologies (2012) [15].

2.3. *Synthesis of Schiff base ligands*

All tetradentate Schiff bases were prepared by condensation of diamine (1 mM, in 20 ml methanol) and hydroxyaldehydes (2 mM, in 20 ml methanol), and were purified by recrystallization from a dichloromethane/hexane mixed solvent through the partial evaporation of the more volatile dichloromethane [16]. All Schiff bases were dried at 50 °C in vacuum.

2.3.1. N,N′-bis(salicyliden)-2,3-diaminopyridine (salpyr). Yield: 54%, Color: Yellow, m.p. 145 °C. Anal. Calcd for $C_{19}H_{15}N_3O_2$ (%): C, 71.91; H, 4.76; N, 13.24. Found: C,

71.56; H, 4.50; N, 13.31. ^{1}H NMR (250 MHz, CDCl$_3$, room temperature): δ(ppm) = 6.94–7.54 (m, 10H, Ar–H, pyridine-H), 8.40 (d, 1H, pyridine–H^{10}), 8.65 (s, 1H, H$^{7'}$), 9.90 (s, 1H, H^7), 12.82 (s, 1H, OH^b), 13.35 (s, 1H, OH^a). IR (KBr, cm^{-1}): 3448 (ν_{O-H}), 2850–3047 (ν_{C-H}), 1620 ($\nu_{C=N}$), 1558 ($\nu_{C=C}$), 1272 (ν_{C-O}). UV–vis. (acetonitrile): λ_{max} (nm), ε (M^{-1} cm^{-1}) = 205(~3402), 271(~29,570), 337(~24,940).

2.3.2. N,N′-bis(3-methoxysalicylidene)-2,3-diaminopyridine (3-MeOsalpyr). Yield: 58%, Color: orange, m.p. 222 °C. Anal. Calcd for C$_{21}$H$_{19}$N$_3$O$_4$ (%): C, 66.83; H, 5.07; N, 11.13. Found: C, 66.45; H, 4.76; N, 11.32. ^{1}H NMR (250 MHz, DMSO, room temperature): δ(ppm) = 3.82 (s, 6H,OCH$_3$), 6.86–7.91 (m, 8H, Ar–H, pyridine–H), 8.41 (s, 1H, pyridine–H^{10}), 8.95 (s, 1H, H$^{7'}$), 9.51 (s, 1H, H^7), 12.57 (s, 1H, OH^b), 13.19 (s, 1H, OH^a). IR (KBr, cm^{-1}): 3448 (ν_{O-H}), 2831–3025 (ν_{C-H}), 1612 ($\nu_{C=N}$), 1558 ($\nu_{C=C}$), 1242 (ν_{C-O}). UV–vis. (acetonitrile): λ_{max} (nm), ε (M^{-1} cm^{-1}) = 224(~28,903), 284(~24,780), 308(~23,468).

2.3.3. N,N′-bis(5-methoxysalicylidene)-2,3-diaminopyridine (5-MeOsalpyr). Yield: 61%, Color: red, m.p. 140 °C. Anal. Calcd for C$_{21}$H$_{19}$N$_3$O$_4$ (%): C, 66.83; H, 5.07; N, 11.13. Found: C, 66.98; H, 4.88; N, 11.17. ^{1}H NMR (250 MHz, DMSO, room temperature): δ(ppm) = 3.82 (s, 6H, OCH$_3$), 6.89–7.54 (m, 8H, Ar–H, pyridine–H), 8.40 (s, 1H, pyridine–H^{10}), 8.60 (s, 1H, H$^{7'}$), 9.86 (s, 1H, H^7), 12.38 (s, 1H, OH^b), 12.92 (s, 1H, OH^a). IR (KBr, cm^{-1}): 3400 (ν_{O-H}), 2831–3020 (ν_{C-H}), 1612 ($\nu_{C=N}$), 1589 ($\nu_{C=C}$), 1265 (ν_{C-O}). UV–vis. (acetonitrile): λ_{max} (nm), ε (M^{-1} cm^{-1}) = 239(~57,835), 273(~29,502), 331(~23,033), 368(~21,174).

2.3.4. N,N′-bis(5-chlorosalicylidene)-2,3-diaminopyridine (5-Clsalpyr). Yield: 64%, Color: yellow, m.p. 144 °C. Anal. Calcd for C$_{19}$H$_{13}$Cl$_2$N$_3$O$_4$ (%): C, 59.09; H, 3.39; N, 10.88. Found: C, 58.85; H, 3.19; N, 11.26. ^{1}H NMR (250 MHz, CDCl$_3$, room temperature, TMS): δ(ppm) = 6.99–7.55 (m, 8H, Ar–H, pyridine–H), 8.46 (d, 1H, pyridine–H^{10}), 8.58 (s, 1H, H$^{7'}$), 9.47 (s, 1H, H^7), 12.77 (s, 1H, OH^b), 13.35 (s, 1H, OH^a). IR (KBr, cm^{-1}): 3433 (ν_{O-H}), 2990–3020 (ν_{C-H}), 1620 ($\nu_{C=N}$), 1551 ($\nu_{C=C}$), 1265 (ν_{C-O}).

2.3.5. N,N′-bis(5-bromosalicylidene)-2,3-diaminopyridine(5-Brsalpyr). Yield: 86%, Color: yellow, m.p. 228 °C. Anal. Calcd for C$_{21}$H$_{19}$N$_3$Br$_2$O$_4$ (%): C, 48.04; H, 2.76; N, 8.84. Found: C, 48.16; H, 2.88; N, 8.78. ^{1}H NMR (250 MHz, DMSO, room temperature): δ(ppm) = 6.91–8.04 (m, 8H, Ar-H), 8.92 (d, 1H, pyridine–H^{10}), 9.51 (s, 1H, H$^{7'}$), 10.18 (s, 1H, H^7), 12.64 (s, 1H, OH^b), 13.15 (s, 1H, OH^a). IR (KBr, cm^{-1}): 3463 (ν_{O-H}), 2920–3160 (ν_{C-H}), 1589 ($\nu_{C=N}$), 1551 ($\nu_{C=C}$), 1265 (ν_{C-O}). UV–vis. (acetonitrile): λ_{max} (nm), ε (M^{-1} cm^{-1}) = 232(~38,978), 269(~20,593), 348(~17,934).

2.4. *Synthesis of uranyl complexes*

Uranyl complexes (figure 1) were prepared by addition of uranyl acetate dihydrate (5 mM in 20 ml methanol) to a hot methanolic solution (20 ml) of the Schiff base (5 mM) (1:1 M ratio), except for 4-methoxysalpyr complex that was synthesized with a template method. The color of the solution changed to orange–red in a few minutes. The mixture was then refluxed for 3 h. The solid was washed with ether, followed by drying at 50 °C in vacuum.
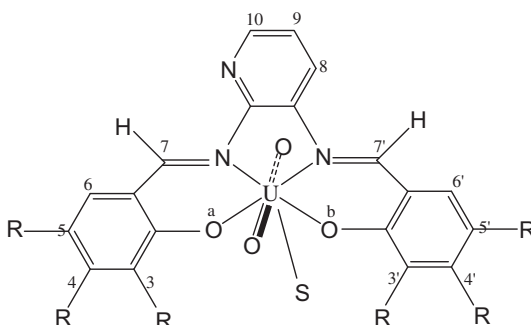
Figure 1. Structural representation of the uranyl(VI) Schiff base complex. 5,5′: R = H (salpyr), R = OMe (5-MeOsalpyr), R = Cl (5-Clsalpyr), R = Br (5-Clsalpyr); 4,4′; R = OMe (4-MeOsalpyr), 3,3′; R = OMe (3-MeO-salpyr), and S = solvent.

2.4.1. [UO₂(salpyr)(MeOH)]. Yield: 85%, Color: red, m.p. > 300 °C, Anal. Calcd for $C_{19}H_{13}N_3O_4U$ (%): C, 38.91; H, 2.78; N, 6.81. Found: C, 38.52; H, 2.54; N, 6.65. ^1H NMR (250 MHz, DMSO-d_6, room temperature): δ (ppm) = 3.15 (s, 3H, MeOH), 4.13 (q, 1H, MeOH), 6.70–8.32 (m, 10H, Ar–H, pyridine–H), 8.57 (d, 1H, pyridine–H^{10}), 9.67 (s, 1H, $H^{7'}$), 10.17 (s, 1H, H^7). IR (KBr, cm^{-1}): 3417 (υ_{O-H}, CH_3OH), 2746–3001 (υ_{C-H}), 1604 ($\upsilon_{C=N}$), 1535 ($\upsilon_{C=C}$), 1203 (υ_{C-O}), 902 ($\upsilon_{U=O}$), 540 (υ_{U-N}), 440 (υ_{U-O}). UV–vis. (acetonitrile): λ_{max} (nm), ε (M^{-1} cm^{-1}) = 239(~34,281), 283(~25,631), 338(~16,179), 411 (~10,985). CV(V): −0.784(E_{pa}), −1.010(E_{pc}).

2.4.2. [UO₂(3-MeOsalpyr)(MeOH)]·0.8H₂O. Yield: 77%, Color: orange, m.p. > 300 °C, Anal. Calcd for $C_{21}H_{17}N_3O_6U$ (%): C, 38.19; H, 3.29; N, 6.07. Found: C, 37.75; H, 3.02; N, 5.99. ^1H NMR (250 MHz, DMSO, room temperature): δ (ppm) = 3.15 (d, 3H, MeOH), 4.10 (q, 1H, MeOH), 3.97 (s, 6H, OCH_3), 6.67 (d, 2H, Ar–$H^{4,4'}$), 7.27 (d, 2H, Ar–$H^{6,6'}$), 7.44 (dd, 2H, Ar–$H^{5,5'}$), 7.58 (dd, 1H, pyridine–H^9), 8.30 (d, 1H, pyridine–H^8), 8.56 (d, 1H, pyridine–H^{10}), 9.65 (s, 1H, $H^{7'}$), 10.15 (s, 1H, H^7). IR (KBr, cm^{-1}): 3421 (υ_{O-H}, MeOH), 2922–3068 (υ_{C-H}), 1602 ($\upsilon_{C=N}$), 1544 ($\upsilon_{C=C}$), 1207 (υ_{C-O}), 902 ($\upsilon_{U=O}$). UV–vis. (acetonitrile): λ_{max} (nm), ε (M^{-1} cm^{-1}) = 244(~36,364), 357(~20,099), 444(sh). CV(V): −0.788(E_{pa}), −1.001(E_{pc}).

2.4.3. [UO₂(4-MeOsalpyr)(MeOH)]. This complex was synthesized by template method. Yield: 78%, Color: orange, m.p. > 300 °C, Anal. Calcd for $C_{21}H_{17}N_3O_6U$ (%): C, 39.01; H, 3.12; N, 6.20. Found: C, 38.60; H, 3.00; N, 6.09. ^1H NMR (250 MHz, DMSO-d_6, room temperature): δ (ppm) = 3.1 (d, 3H, MeOH), 4.1 (q, 1H, MeOH), 3.9 (s, 6H, OCH_3), 6.4 (d, 2H, Ar–$H^{5,5'}$), 6.5 (s, 2H, Ar–$H^{3,3'}$), 7.5 (dd, 1H, pyridine H^9), 7.7 (d, 1H, Ar–H^6), 7.8 (d, 1H, Ar–$H^{6'}$), 8.2 (d, 1H, pyridine–H^8), 8.5 (d, 1H, pyridine–H^{10}), 9.5 (s, 1H, $H^{7'}$), 10.0 (s, 1H, H^7). IR (KBr, cm^{-1}): 3425 (υ_{O-H}), 2900–3070 (υ_{C-H}), 1597 ($\upsilon_{C=N}$), 1519 ($\upsilon_{C=C}$), 1211 (υ_{C-O}), 903 ($\upsilon_{U=O}$), 532 (υ_{U-N}), 447 (υ_{U-O}). UV–vis. (acetonitrile): λ_{max} (nm), ε (M^{-1} cm^{-1}): 217(~24,621), 257(~26,371), 313(~19,648), 357(~20,682), 432(sh). CV(V): −0.791(E_{pa}), −0.972(E_{pc}).

2.4.4. [UO$_2$(5-MeOsalpyr)(MeOH)]. Yield: 90%, Color: orange, m.p. > 300 °C, Anal. Calcd for C$_{21}$H$_{17}$N$_3$O$_6$U (%): C, 39.01; H, 3.12, N; 6.20. Found: C, 38.62; H, 2.80; N, 5.94. ^{1}H NMR (250 MHz, DMSO−d$_6$, room temperature): δ (ppm) = 3.13 (d, 3H, MeOH), 4.12 (q, 1H, MeOH), 3.75 (s, 6H, OCH$_3$), 6.93 (s, 2H, Ar–H$^{6,6'}$), 7.34 (m, 3H, Ar–H), 7.46 (d, 1H, pyridine–H^8), 7.58 (dd, 1H, Ar–H^9), 8.27 (d, 1H, Ar–H), 8.56 (d, 1H, pyridine–H^{10}), 9.63 (s, 1H, H$^{7'}$), 10.14 (s, 1H, H^7). IR (KBr, cm^{-1}): 3417 (υ_{O-H}), 2815–3020(υ_{C-H}), 1589 ($\upsilon_{C=N}$), 1535 ($\upsilon_{C=C}$), 1226 (υ_{C-O}), 902($\upsilon_{U=O}$), 530(υ_{U-N}), 430(υ_{U-O}). UV–vis. (acetonitrile): λ_{max} (nm), ε (M^{-1} cm^{-1}): 249(~37,206), 343(~21,069), 430(sh). CV(V): –0.796 (E$_{pa}$), −1.010(E$_{pc}$).

2.4.5. [UO$_2$(5-Clsalpyr)(MeOH)]. Yield: 86%, Color: orange, m.p. > 300 °C, Anal. Calcd for C$_{19}$H$_{11}$N$_3$O$_4$Cl$_2$U (%): C, 34.88; H, 2.20; N, 6.12. Found: C, 34.74; H, 1.84; N, 5.96. ^{1}H NMR (250 MHz, DMSO-d$_6$, room temperature): δ (ppm) = 3.13 (d, 3H, MeOH), 4.11 (q, 1H, MeOH), 7.02 (s, 2H, Ar–H^6), 7.64 (m, 3H, Ar–H, pyridine–H), 7.88 (d, 1H, Ar–H), 8.01 (d, 1H, Ar–H), 8.34 (dd, 1H, pyridine–H^9), 8.61 (d, 1H, pyridine–H^{10}), 9.66 (s, 1H, H$^{7'}$), 10.14 (s, 1H, H^7). IR (KBr, cm^{-1}): 3380 (υ_{O-H}, MeOH), 2995–3020 (υ_{C-H}), 1598 ($\upsilon_{C=N}$), 1558 ($\upsilon_{C=C}$), 1167 (υ_{C-O}), 900 ($\upsilon_{U=O}$), 563 (υ_{U-N}), 455 (υ_{U-O}). UV–vis. (acetonitrile): λ_{max} (nm), ε (M^{-1} cm^{-1}): 245(~14,493), 290(sh), 338(~13,450), 390(sh). CV(V): −0.784(E$_{pa}$), −1.023(E$_{pc}$).

2.4.6. [UO$_2$(5-Brsalpyr)(MeOH)]. Yield: 86%, Color: orange, m.p. > 300 °C, Anal. Calcd for C$_{19}$H$_{11}$N$_3$O$_4$Br$_2$U (%): C, 30.85; H, 1.95; N, 5.42. Found: C, 30.95; H, 1.66; N, 5.36. ^{1}H NMR (250 MHz, DMSO−d$_6$, room temperature): δ (ppm) = 3.14 (d, 3H, MeOH), 4.10 (q, 1H, MeOH), 6.97–8.30 (d, 8H, Ar–H), 8.58 (d, 1H, pyridine–H^{10}), 9.62 (s, 1H, H$^{7'}$), 10.10 (s, 1H, H^7). IR (KBr, cm^{-1}): 3394 (υ_{O-H}, MeOH), 2920–3010 (υ_{C-H}), 1596 ($\upsilon_{C=N}$), 1566 ($\upsilon_{C=C}$), 1172 (υ_{C-O}), 918 ($\upsilon_{U=O}$), 640 (υ_{U-N}), 446 (υ_{U-O}). UV–vis. (acetonitrile): λ_{max} (nm), ε (M^{-1} cm^{-1}): 245(~50,274), 274(~25,772), 361(~21,994). CV(V): –0.784(E$_{pa}$), −1.003(E$_{pc}$).

2.5. *Kinetic studies of exchange reactions*

The kinetics of exchange reactions on the uranyl center were studied. Kinetic data were determined spectrophotometrically. In all the cases (runs from 10.0–40.0 ± 0.1 °C), the procedure involves adding a sample of PBu$_3$, under pseudo-first-order conditions, to a solution containing the uranyl complex. The kinetics were followed at a predetermined wavelength, where the difference in absorption between the substrate and product was high. After each injection the absorbance was read with definite time intervals [11–14].

2.6. *Synthesis of the kinetic product*

To a refluxing solution of [UO$_2$(salpyr)(solvent)] (0.1 g, 0.017 mM) in acetonitrile (25 ml) was added tri-*n*-butylphosphine (0.042, 0.017 mM) (1 : 1 M ratio). The reaction mixture was refluxed for 24 h under nitrogen. The resulting oil was grounded with *n*-hexane to extract the impurities, and finally a powdery product was obtained [11–14]. ^{1}H NMR spectra of the ligand, uranyl complex, and kinetic product are shown in Supplementary material.

2.6.1. [UO$_2$(salpyr)(PBu$_3$)]·H$_2$O. Yield: 87%, Color: orange, m.p. < 50 °C, Anal. Calcd for C$_{31}$H$_{40}$N$_3$O$_4$PU (%): C, 46.21; H, 5.25; N, 5.22. Found: C, 45.89; H, 5.02; N, 5.48. ^{1}H NMR (250 MHz, DMSO-d$_6$, room temperature): δ (ppm) = 0.8 (t, 9H, CH$_3$), 1.3 (m, 12H, CH$_2$), 1.6 (t, 6H, CH$_2$), 6.7–8.3 (m, 10H, Ar–H, pyridine–H), 8.6 (d, 1H, pyridine–H^{10}), 9.7 (s, 1H, H$^{7'}$), 10.2 (s, 1H, H^7). IR (KBr, cm^{-1}): 2869–3056 (υ_{C-H}), 1604 ($\upsilon_{C=N}$), 1535 ($\upsilon_{C=C}$), 1188 (υ_{C-O}), 895 ($\upsilon_{U=O}$), 540 (υ_{U-N}), 439 (υ_{U-O}). UV–vis. (acetonitrile): λ_{max} (nm), ε (M^{-1} cm^{-1}): 281(~65,750), 353(~53,333), 435(sh).

2.7. *X-ray crystallography*

Red single crystals of [UO$_2$(3-MeOsalpyr)(DMF)] were obtained in good yield, from slow diffusion of diethyl ether into a solution of the metal complex in DMF at room temperature during 10 days. The crystals were intensely colored. The preparation from DMF/Et$_2$O gave better single crystals when compared with preparation from acetonitrile, which was also attempted. The data were collected on a Gemini diffractometer with an Atlas CCD detector using graphite monochromated Mo Kα radiation (λ = 0.7107 Å) and corrected for absorption using CrysAlisPro software. The structure was solved by the charge-flipping method using Superflip [17] and refined by full matrix least squares on F^2 with the JANA2006 program [15]. The disordered solvent molecules were determined as rigid bodies in close positions described by a refined translation vector and three rotations.

2.7.1. [UO$_2$(3-MeOsalpyr)(DMF)]. Color: deep red, m.p. = 150 °C, Anal. Calcd for C$_{24}$H$_{24}$N$_4$O$_7$U (%): C, 40.12; H, 3.37; N, 7.80. Found: C, 40.19; H, 3.32; N, 7.98. ^{1}H NMR (250 MHz, DMSO-d$_6$, room temperature): δ (ppm) = 2.77 (s, 3H, CH$_3$-DMF), 2.93 (s, 3H, CH$_3$-DMF), 3.93 (s, 6H, OCH$_3$), 6.62–7.60 (m, 7H, Ar, pyridine), 8.01 (s, 1H, DMF), 8.27 (d, 1H, pyridine-H^8), 8.52 (d, 1H, pyridine-H^{10}), 9.65 (s, 1H, H$^{7'}$), 10.15 (s, 1H, H^7). IR (KBr, cm^{-1}): 2922–3068 (υ_{C-H}), 1643 ($\upsilon_{C=O}$), 1602 ($\upsilon_{C=N}$), 1544 ($\upsilon_{C=C}$), 1207 (υ_{C-O}), 902 ($\upsilon_{U=O}$). UV–vis. (DMF): λ_{max} (nm), ε (M^{-1} cm^{-1}) = 242(~36,364), 354 (~20,099), 442(sh).

3. Results and discussion

3.1. *Characterization of the complexes*

3.1.1. Crystal structure of [UO$_2$(3-MeOsalpyr)(DMF)]. Crystallographic data and details of the data collection are listed in table 1. The ORTEP view of this complex is shown in figure 2, with selected bonding parameters listed in table 2.

The uranium was coordinated as a distorted pentagonal bipyramid with uranyl oxygens located in the axial positions. Four equatorial positions were occupied by two nitrogens and two oxygens of the tetradentate Schiff base, while the fifth position was DMF. Both the molecules of DMF – the coordinated one as well as the free one – were disordered. The coordination geometry around UO$_2$ was nearly planar with the dihedral angle of 2.56(16)° between the coordination planes of N16–U1–O24 and N9–U1–O1. C10 and C15 belonging to the aromatic rings were out of the equatorial plane, with a distance from the plane 0.449(4) Å for C10 and 0.466(4) Å for C15. The U=O bond distances in uranyl were 1.781

Table 1. Crystal data, data collection and structure refinement details for [UO$_2$(3-MeO salpyr)(DMF)].

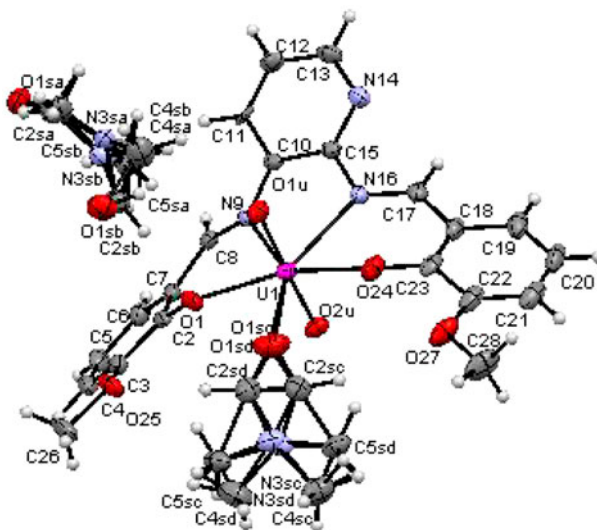|	Complex
Formula	C$_{27}$H$_{31}$N$_5$O$_8$U
Formula weight	791.60
Crystal system	Triclinic
Hall group	$-P-1$
Space group	$P-1$
T [K]	120
a [Å]	9.4402(3)
b [Å]	10.9098(5)
c [Å]	14.6683(5)
α [°]	106.42(3)
β [°]	92.92(3)
γ [°]	103.56(3)
V [Å^3]	1397.53(10)
Z	2
D_{Calcd} [Mg m^{-3}]	1.88
F (000)	768.0
Nref	7722[6820]
T_{min}, T_{max}	0.043, 0.563
R(reflections > 3σ)	0.0295(5769)
wR2(all reflections)	0.0625(6820)

Figure 2. ORTEP view of [UO$_2$(3-MeOsalpyr)(DMF)].

(3) Å for U1–O1u and 1.783(3) Å for U1–O2u, typical values for uranyl compounds [1, 14]. The O1u–U1–O2u bond angle 175.83(13)° indicated that uranyl was slightly bent in the direction opposite to coordinated DMF. The U1–O1 and U1–O24 bond distances 2.245 (3) and 2.246(3) Å, respectively, were shorter than U1–N9 and U1–N16 [2.537(3), 2.573 (3) Å]. Such a difference might imply that coordination of oxygen in the complex was stronger than coordination of nitrogen. The bond distance between oxygen of DMF and

Table 2.   Selected bond distances (Å) and angles (°) for [UO$_2$(3-MeOsalpyr)(DMF)].

U1–O1u	1.781(3)	O1u–U1–O2u	175.83(13)
U1–O2u	1.783(3)	O1u–U1–O1sc	93.6(2)
U1–O24	2.246(3)	O1u–U1–O1sd	94.5(5)
U1–O1	2.245(3)	O24–U1–N16	70.23(10)
U1–O1sc	2.399(7)	O1–U1–N9	69.89(10)
U1–O1sd	2.310(2)	N9–C10–C15–N16	−0.7(5)
U1–N9	2.537(3)	N16–C17–C18–C23	−12.0(7)
U1–N16	2.573(3)	N9–C8–C7–C2	14.9(7)

uranium was 2.399(6) Å [U1–O1sc], longer than those of U1–O1 and U1–O24, suggesting that coordination of DMF was not as strong as coordination of the Schiff base.

3.1.2. ^{1}H NMR spectroscopy. In ^{1}H NMR spectra of the ligands, because of the unsymmetrical structure, two singlets for methine (HC=N) protons and two singlets for hydroxyl protons were present. In ^{1}H NMR spectra of the complexes a significant shift in the imine proton was observed (9.54–10.17 ppm) as compared to the free ligand (8.65–9.90 ppm), indicative of the imine nitrogen lone pairs coordinating. Also the absence of hydroxyl protons at ~12 ppm showed that the Schiff base was coordinated to the metal. ^{1}H NMR spectra of the complexes showed a differentiation of almost all hydrogens [18], since they were in different chemical environments due to the rigid structure of the ligand coordinated to the metal [19]. The formation of rigid structure also supports the visibility of aromatic protons. In spectra of complexes, two sets of resonances were observed for azomethine proton, confirming their different chemical environments. The proton chemical shifts of the coordinated PBu$_3$ in the kinetic product appear at $\delta = 0.8$–1.6 ppm, in agreement with previous results observed for metal complexes with tributylphosphine as ligand [20, 21].

By considering the crystal structure of UO$_2$(salophen)DMF [6], it is clear that one solvent molecule, which was used in the crystallization, is coordinated to the uranium and the complex has a pentagonal-bipyramidal geometry with axial O=U=O. Comparing bond distances shows that U–O(salophen) bond distances are shorter than U–N(salophen). The bond distance between the oxygen of DMF and uranium is the longest, suggesting that coordination of DMF is not as strong as coordination of salophen. The solvent in the fifth position of the equatorial plane depends on the solvent used for synthesis or crystallization; changing the solvent of the synthesis or crystallization changes the coordinated solvent [10].

All ^{1}H NMR of the complexes were recorded in DMSO-d$_6$ solvent, and it is expected that DMSO-d$_6$ replaced methanol in the coordination sphere. Peaks due to free MeOH were observed in the ^{1}H NMR as a quartet at 4.12 ppm related to OH and a doublet at 3.15 ppm from CH$_3$. In ^{1}H NMR spectra of [UO$_2$(3-MeOsalpyr)(DMF)] signals of methyl and formyl of DMF were observed at 2.93, 2.77 and 8.01 ppm, respectively.

3.1.3. IR spectroscopy. IR spectra of the ligands exhibited broad medium intensity bands at 3400–3463 cm^{-1} were assigned to the intramolecular hydrogen bonding vibration (O–H···N) [22]. These bands should disappear due to complexation, but because of the existence of methanol in our complexes, we could see these bands after complexation. In

the IR spectrum of [UO$_2$(3-MeOsalpyr)(DMF)], these bands were not present but a band due to C=O of DMF was at 1643 cm^{-1}. The vibration of azomethine of free ligand was at 1589–1620 cm^{-1}. In the complexes, these bands shifted to lower frequencies (1589–1602 cm^{-1}), indicating that nitrogen of azomethine coordinated [23, 24]. Coordination of azomethine nitrogen was affirmed by the presence of new bands at 530–640 cm^{-1}, assignable to υ_{U-N}. A new band at 430–455 cm^{-1} for the complexes was assignable to υ_{U-O}. The characteristic uranyl $\upsilon_{U=O}$ appeared at 902–918 cm^{-1}. In [UO$_2$(salpyr)(PBu$_3$)], the bands around 2869–3050 cm^{-1} were stronger due to coordination of PBu$_3$.

3.1.4. UV–vis spectra. Electronic spectra of salpyr and its complex in acetonitrile are shown in figure 3. The electronic spectra of the ligands have three intense bands. The first band at higher energy is attributed to $\pi \to \pi^*$ transition of the phenyl ring, the band at lower energy from $\pi \to \pi^*$ transition of the azomethine chromophore, and the lowest energy band was $n \to \pi^*$ transition of lone pair electrons of nitrogen to the antibonding π^* orbital. Usually $n \to \pi^*$ transition involving nitrogen occurs at low energies.

The intense absorption bands of the complexes assigned to an electric dipole allowed transition arising from the coordinating ligand and/or from charge transfer between ligand and uranium. Owing to the presence of phenolate, these ligands could act as electron donors. Since U(VI) has an empty valence shell, the metal can function as acceptor for LMCT transitions. Charge transfer (LMCT) from oxide (=O) to uranyl occurred at lower frequencies (higher wavelengths) than the Schiff base^{2-}→U(VI) [5].

3.1.5. Thermal analysis. During thermal analysis, heating rates were set to 20 °C min^{-1} under nitrogen and the weight loss was measured from ambient temperature to 1000 °C. Thermogravimetric analysis showed that uranyl complexes had very different thermal stabilities. This method also established that only one solvent molecule was coordinated to the central uranium and this solvent did not coordinate strongly. Because these complexes were synthesized in methanol, we expected that one methanol was coordinated and it was confirmed by investigating the TG and TGA curves (figure 4). All thermal data are collected in table 3.
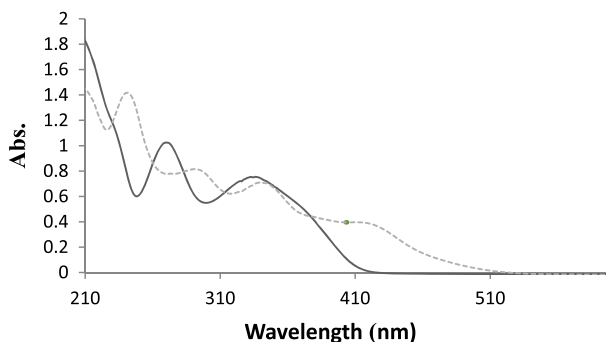

Figure 3. The electronic spectra of H$_2$salpyr (dark), [UO$_2$(salpyr)(CH$_3$CN)](light), in acetonitrile.
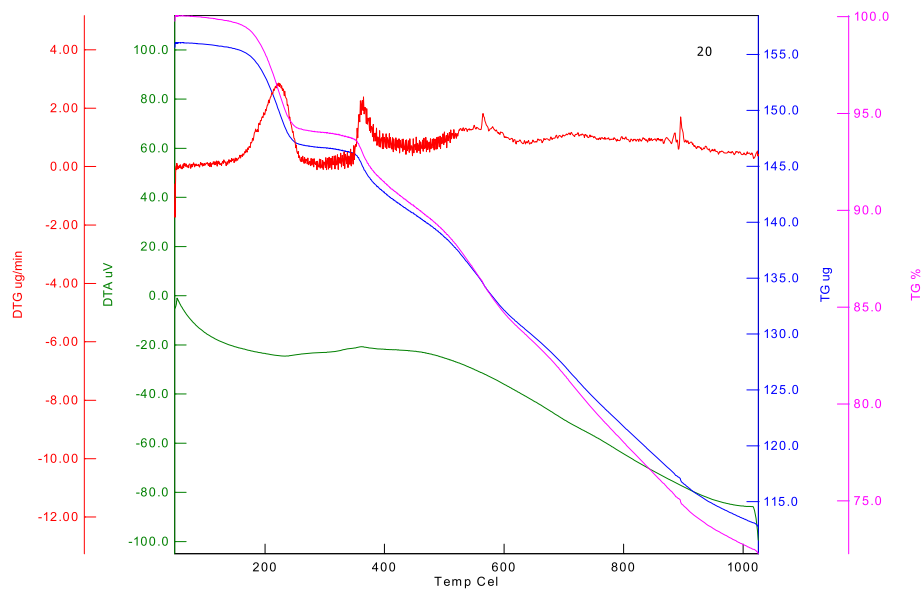
Figure 4.   TG and DTG and DTA diagram of [UO_2(salpyr)(MeOH)].

Table 3.   Thermal analyzes data for uranyl Schiff base complexes.

Complex (MW)	(Wt. loss %) Calcd (found)	Temp. range in TG (°C)	DTA (peak) endo/exo	Decomposition assignment
[UO_2(salpyr)(MeOH)]	5.2 (6.0)	100–278	Endo	Loss of MeOH
$C_{20}H_{17}N_3O_5U$	12.5 (10.3)	316–607	Exo	Loss of C_5NH_3
(617.40)				
[UO_2(3-MeOsalpyr)	2.1 (2.0)	44–98	Endo	Loss of H_2O
(MeOH)]·0.8H_2O	4.6 (3.5)	100–200	Endo	Loss of MeOH
$C_{22}H_{21}N_3O_7U$	19.1 (19.5)	200–747	Exo	Loss of $C_7N_3H_5$
(691.85)				
[UO_2(4-MeOsalpyr)(MeOH)]	4.7 (4.0)	108–190	Endo	Loss of MeOH
$C_{22}H_{21}N_3O_7U$				
(677.45)				
[UO_2(5-MeOsalpyr)(MeOH)]	4.7 (5.0)	105–292	Endo	Loss of MeOH
$C_{22}H_{21}N_3O_7U$				
(677.45)				
[UO_2(5-Brsalpyr)(MeOH)]	4.3 (3.2)	102–288	Endo	Loss of MeOH
$C_{17}H_{16}N_2O_5Br_2U$				
(742.8)				
[UO_2(5-Clsalpyr)(MeOH)]	4.6 (5.5)	120–289	Endo	Loss of MeOH
$C_{18}H_{20}N_2O_5U$	11.2 (7.0)	322–423	Exo	Loss of C_5NH_3
(686.29)				

3.2. *The electrochemical study of uranyl complexes*

In order to investigate the effect of substituents of the Schiff base on the oxidation and reduction potentials of [UO_2(L)(CH_3CN)], uranyl Schiff base complexes were studied by cyclic voltammetry. Cyclic voltammetry measurements for uranyl complexes in acetonitrile (1×10^{-3} M) and TBAP (tetrabutylammoniumperchlorate) (0.10 M) as the supporting electrolyte were carried out at room temperature from −0.65 to −1.28 V at scan rates

V = 0.1 V/s. Typical cyclic voltammograms of $[UO_2(L)(CH_3CN)]$ in the potential range from 0.0 to −1.3 V (*versus* Ag/AgCl) are shown in figure 5. A reduction peak observed at ca. −1.00 V with $[UO_2(L)(CH_3CN)]$, reduced to the mono anion $[UO_2(L)(CH_3CN)]^-$ in a quasi-reversible one electron step (Equation 1).

$$[U^{VI}O_2(L)CH_3CN] + e \rightarrow [U^{V}O_2(L)CH_3CN]^- \tag{1}$$
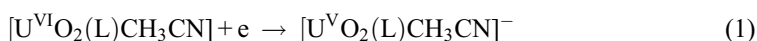
Upon reversal of the scan direction, the U(V) complex was oxidized to U(VI) at over potentials. The oxidation potentials for the different complexes are collected in table 4. The formal potentials ($E_{1/2}(VI \leftrightarrow V)$) for the U(V/VI) redox couple were calculated as the average of the cathodic (E_{pc}) and anodic (E_{pa}) peak potentials of this process.

The cathodic peak potentials increased 5-MeO < 3-MeO < 4-MeO. Methoxy para- (5-MeO) and ortho- (3-MeO) were electron releasing, while a methoxy meta- (4-MeO) was a weaker electron releasing group. This accelerated reduction of 4-MeO related to 5-MeO and 3-MeO.

3.3. *Kinetic study of the solvent exchange with PBu₃ on uranium center*

The kinetics of the interaction between the uranyl Schiff base complexes and PBu$_3$ were studied (Equation 2).
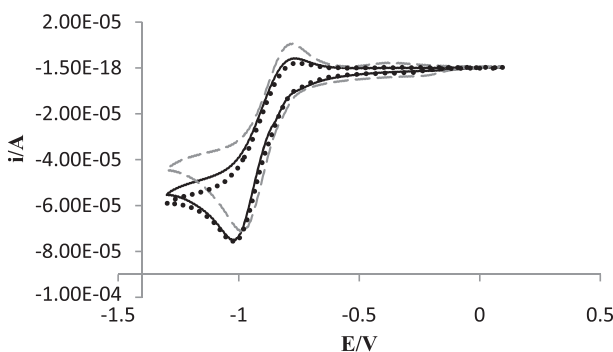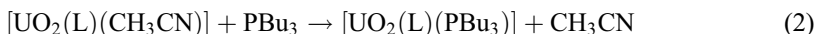
$$[UO_2(L)(CH_3CN)] + PBu_3 \rightarrow [UO_2(L)(PBu_3)] + CH_3CN \tag{2}$$

Figure 5. Cyclic voltammograms of $[UO_2(L)(CH_3CN)]$, where L = 3-MeOsalpyr(—), 4-MeOsalpyr(– –), 5-MeOsalpyr(….), in acetonitrile at room temperature. Scan rate: 0.1 V/s.

Table 4. Redox potential data of uranyl complexes in acetonitrile solution.

Compound	$E_{pa(V \rightarrow VI)}$	$E_{pc(VI \rightarrow V)}$	$E_{1/2(V \leftrightarrow VI)}$
$[UO_2(salpyr)(CH_3CN)]$	−0.784	−1.010	−0.897
$[UO_2(3\text{-}MeOsalpyr)(CH_3CN)]$	−0.788	−1.001	−0.894
$[UO_2(4\text{-}MeOsalpyr)(CH_3CN)]$	−0.791	−0.972	−0.881
$[UO_2(5\text{-}MeOsalpyr)(CH_3CN)]$	−0.769	−1.010	−0.889
$[UO_2(5\text{-}Brsalpyr)(CH_3CN)]$	−0.784	−1.003	−0.893
$[UO_2(5\text{-}Clsalpyr)(CH_3CN)]$	−0.784	−1.023	−0.903

By dissolving the complexes in acetonitrile, methanol was exchanged with acetonitrile, thus acetonitrile occupied the fifth position in the equatorial plane. Plots of k_{obs} *versus* [PBu$_3$] exhibited a nonzero intercept. Thus the rate-law for the reaction was (Equations 3–5):

$$R = \{k_1 + k_2[PBu_3]\}[complex] \qquad (3)$$

under pseudo-first-order conditions:

$$R = k_{obs}[complex] \qquad (4)$$

where

$$k_{obs} = k_1 + k_2[PBu_3] \qquad (5)$$

k_2 is the second-order rate constant (scheme 1, Path 1) and k_1 is the first-order rate constant (scheme 1, Path 2).

The rate constants and the activation parameters are collected in tables 5–11. The mechanism shown in scheme 1 was suggested for the reaction of uranyl complex with PBu$_3$.

Two paths were suggested for the reaction. In Path 1, PBu$_3$ was added to the uranium center by an associative mechanism with a rate constant k_2, with the suggested structures shown in scheme 1. An eight-coordinate intermediate was formed and then dissociation of the solvent gave a seven-coordinate product. In Path 2 (a dissociative path) with k_1 rate constant a six-coordinate intermediate was formed and PBu$_3$ coordinated to uranium in the fast step.

Variation of the electronic spectra for [UO$_2$(salpyr)(CH$_3$CN)] reacting with an excess of PBu$_3$ at 10 °C is shown in figure 6.

The k_2 values were obtained from the slope of linear plots of k_{obs} *versus* the donor concentration [PBu$_3$] and the k_1 values were obtained from their intercept (figure 7).

The activation parameters of the studied systems were calculated by using the Eyring Equation (6):

$$\ln(k_2/T) = -\Delta H^{\#}/RT + \Delta S^{\#}/R + 23.8 \qquad (6)$$
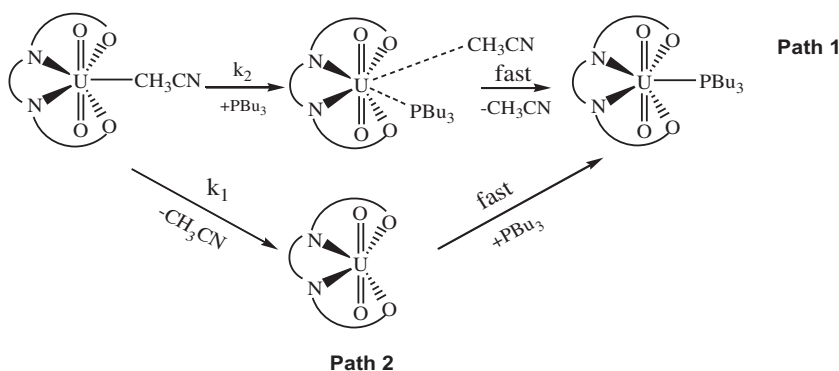
Scheme 1.   Suggested paths for the reaction mechanism.

Table 5. Pseudo-first-order rate constants, $10^3 k_{obs}^a$ (s^{-1}), k_1^a (s^{-1}), k_2^a (M^{-1} s^{-1}), for the reaction of [UO$_2$(3-OMesalpyr)(CH$_3$CN)] with PBu$_3$ in acetonitrile at different temperatures. [Complex] = 2.5×10^{-5} M.

10^3[PBu$_3$]/M (°C)	7.48	14.96	22.44	29.92	37.40	44.88	52.36	59.84	$10^3 k_1$/s^{-1}	$10^1 k_2$/M^{-1} s^{-1}
10	1.4(0.0)	2.3(0.0)	3.1(0.1)	4.7(0.2)	6.1(0.4)	6.7(0.3)	8.0(0.8)	8.5(0.7)	0.3(1.0)	1.4(0.0)
20	2.0(0.0)	3.6(0.0)	4.3(0.1)	5.8(0.2)	7.5(0.8)	8.4(0.3)	9.3(0.8)	10.3(0.4)	1.0(0.2)	1.6(0.1)
30	2.7(0.0)	4.1(0.0)	5.4(0.6)	6.9(0.7)	7.8(1.6)	8.5(0.8)	10.5(1.0)	12.1(1.3)	1.4(0.2)	1.7(0.1)
40	3.7(0.2)	5.4(0.1)	6.2(0.4)	7.1(0.1)	8.9(0.0)	11.5(1.0)	12.7(1.1)	13.7(1.1)	2.3(0.2)	2.0(0.1)

Note: The numbers in parentheses are the standard deviations of k_{obs}.

Table 6. Pseudo-first-order rate constants, $10^3 k_{obs}^a$ (s^{-1}), k_1^a (s^{-1}), k_2^a ($M^{-1} s^{-1}$), for the reaction of [UO_2(5-Clsalpyr)(CH_3CN)] with PBu_3 in acetonitrile at different temperatures. [Complex] = 2.2×10^{-5} M.

$10^3[PBu_3]$/M (°C)	3.0	6.0	9.0	12.0	15.0	18.0	21.0	24.0	$10^3 k_1$/s^{-1}	$10^1 k_2$/M^{-1} s^{-1}
10	2.9(0.0)	3.8(0.0)	4.6(0.1)	5.9(0.0)	7.2(0.1)	8.5(0.3)	9.5(0.2)	10.6(0.3)	1.5(0.2)	3.8(0.1)
20	3.1(0.0)	4.1(0.1)	5.9(0.2)	6.9(0.8)	8.6(0.3)	9.5(0.0)	10.3(0.0)	11.2(0.2)	2.0(0.1)	4.0(0.2)
30	3.1(0.2)	4.4(0.4)	6.0(0.3)	7.2(0.0)	8.7(0.2)	9.8(0.8)	10.6(1.1)	12.2(1.2)	2.0(0.2)	4.2(0.1)
40	3.3(0.3)	4.7(0.3)	6.3(0.5)	7.3(0.7)	8.9(0.6)	10.8(1.0)	11.7(1.1)	12.5(1.1)	2.1(0.5)	4.6(0.1)

Note: The numbers in parentheses are the standard deviations of k_{obs}.

Table 7. Pseudo-first-order rate constants, $10^3 k_{obs}{}^a$ (s^{-1}), $k_1{}^a$ (s^{-1}), $k_2{}^a$ ($M^{-1}\,s^{-1}$), for the reaction of [UO$_2$(5-Brsalpyr)(CH$_3$CN)] with PBu$_3$ in acetonitrile at different temperatures. [Complex] = 2.3×10^{-5} M.

10^3[PBu$_3$]/M (°C)	7.48	14.96	22.44	29.92	37.40	44.88	59.84	$10^3 k_1/s^{-1}$	$10^1 k_2/M^{-1}\,s^{-1}$
10	8.0(0.1)	8.9(0.1)	13.0(0.1)	14.1(0.2)	14.7(0.2)	20.0(0.3)	25.0(0.7)	4.7(1.0)	3.3(0.3)
20	8.1(0.0)		13.5(0.2)	14.3(0.8)	18.3(0.3)	22.1(0.0)		4.9(1.1)	3.6(0.4)
30	8.3(0.2)		13.7(0.3)		19.5(0.2)	23.0(0.8)	29.0(1.2)	5.0(0.3)	4.0(0.0)
40	8.4(0.3)	9.0(0.3)	16.8(0.5)	18.4(0.7)	22.2(0.6)	24.3(1.0)	30.0(1.1)	5.1(1.3)	4.3(0.4)

Note: The numbers in parentheses are the standard deviations of k_{obs}.

Table 8. Pseudo-first-order rate constants, $10^3 k_{obs}{}^a$ (s^{-1}), $k_1{}^a$ (s^{-1}), $k_2{}^a$ ($M^{-1}\,s^{-1}$), for the reaction of [UO$_2$(5-MeOsalpyr)(CH$_3$CN)] with PBu$_3$ in acetonitrile at different temperatures. [Complex] = 3.2×10^{-5} M.

10^3[PBu$_3$]/M (°C)	7.5	15.0	22.5	30.0	37.5	45.0	52.5	60.0	$10^3 k_1/s^{-1}$	$10^2 k_2/M^{-1}\,s^{-1}$
10	1.3(0.0)	1.4(0.1)	1.5(0.2)	1.6(0.2)	1.7(0.4)	1.8(0.5)	1.8(0.7)	1.9(1.0)	1.2(0.0)	1.2(0.3)
20	3.2(0.1)	3.2(0.0)	3.3(0.2)	3.4(0.8)	3.6(0.3)	3.8(0.0)	3.9(0.8)	3.9(0.8)	3.0(0.0)	1.6(0.0)
30	5.1(0.2)	5.2(0.2)	5.5(0.3)	5.6(0.3)	5.8(0.2)	5.9(0.8)	6.1(1.0)	6.1(1.2)	4.9(0.0)	2.1(0.1)
40	8.0(0.3)	8.3(0.3)	8.6(0.5)	8.8(0.7)	9.1(0.6)	9.4(1.0)	9.4(1.0)	9.8(1.1)	7.7(0.0)	3.3(0.1)

Note: The numbers in parentheses are the standard deviations of k_{obs}.

Table 9. Pseudo-first-order rate constants, $10^3 k_{obs}{}^a$ (s^{-1}), $k_1{}^a$ (s^{-1}), $k_2{}^a$ ($M^{-1}\,s^{-1}$), for the reaction of [UO$_2$(4-MeO-salpyr)(CH$_3$CN)] with PBu$_3$ in acetonitrile at different temperatures. [Complex] = 2.9×10^{-5} M.

10^3[PBu$_3$]/M (°C)	7.50	11.25	15.00	18.75	22.50	26.25	30.00	33.75	$10^3 k_1/s^{-1}$	$10^2 k_2/M^{-1}\,s^{-1}$
10	0.8(0.1)	0.8(0.2)	0.8(0.1)	0.9(0.2)	0.9(0.2)	0.9(0.4)	1.5(0.6)	1.0(0.8)	0.7(0.0)	0.8(0.5)
20	1.3(0.0)	5.1(0.3)	1.3(0.2)	1.4(0.8)	1.4(0.3)	5.7(1.0)	3.2(0.9)	3.3(1.2)	1.1(0.0)	1.1(0.0)
30	2.7(0.2)		2.9(0.3)	3.0(0.4)	3.2(0.2)		5.8(0.9)		2.5(0.0)	2.4(0.3)
40	5.0(0.3)	5.1(0.6)	5.2(0.5)		5.5(0.6)	5.7(0.9)			4.7(0.0)	3.8(0.1)

Note: The numbers in parentheses are the standard deviations of k_{obs}.

Table 10. Pseudo-first-order rate constants, $10^3 k_{obs}{}^a$ (s^{-1}), $k_1{}^a$ (s^{-1}), $k_2{}^a$ ($M^{-1}\,s^{-1}$), for the reaction of [UO$_2$(salpyr)(CH$_3$CN)] with PBu$_3$ in acetonitrile at different temperatures. [Complex] = 2.7×10^{-5} M.

10^3[PBu$_3$]/M (°C)	7.5	15.0	22.5	30.0	37.5	45.0	52.5	60.0	$10^3 k_1/s^{-1}$	$10^2 k_2/M^{-1}\,s^{-1}$
10	0.9(0.1)	1.0(0.2)	1.0(0.2)	1.1(0.4)	1.1(0.3)			1.3(1.2)	0.9(0.2)	0.8(0.5)
20	1.5(0.1)	1.5(0.3)	1.6(0.2)	1.7(0.8)		1.9(0.4)	1.5(0.6)	2.1(0.5)	1.3(0.0)	1.4(0.0)
30	2.5(0.2)	2.5(0.1)	2.7(0.3)	2.8(0.5)	2.9(0.2)	3.1(0.7)	3.4(1.0)	3.5(1.2)	2.2(0.0)	2.1(0.3)
40	4.0(0.3)	4.7(0.3)	4.8(0.5)	5.2(0.9)	5.1(0.6)	5.5(1.0)	5.8(0.9)	6.0(0.7)	4.0(1.0)	3.5(0.1)

Note: The numbers in parentheses are the standard deviations of k_{obs}.

A typical linear Eyring plot of $\ln(k_2/T)$ *versus* $1/T$ with a good correlation of 0.97–0.99 at four different temperatures for [UO$_2$(salpyr)(CH$_3$CN)] is shown in figure 8. Also the $\Delta G^{\#}$ values were calculated using Equation (7) at $T = 313$ K.

Table 11. Activation parameters $\Delta H^{\#}$, $\Delta S^{\#}$ and $\Delta G^{\#}$ for the reaction of $[UO_2(L_n)(CH_3CN)]$ with PBu_3 in acetonitrile. The standard deviations are in parentheses.

	$\Delta H^{\#}/kJ\,M^{-1}$	$\Delta S^{\#}/JK^{-1}\,M^{-1}$	$^{a}\Delta G^{\#}/kJ\,M^{-1}$
Salpyr	$3.4\,(0.1) \times 10^{-4}$	$-163.5(4.3)$	$8.7(0.0)$
3-MeOsalpyr	$5.0\,(0.5) \times 10^{-5}$	$-243.4(1.7)$	$4.2(0.1)$
4-MeOsalpyr	$3.8\,(0.4) \times 10^{-4}$	$-151.5(13.8)$	$8.5(0.0)$
5-MeOsalpyr	$2.1\,(0.2) \times 10^{-4}$	$-206.2(8.0)$	$8.9(0.0)$
5-Clsalpyr	$2.0\,(0.2) \times 10^{-5}$	$-254.7(0.5)$	$2.1(0.0)$
5-Brsalpyr	$4.4\,(0.1) \times 10^{-5}$	$-238.7(0.4)$	$2.2(0.1)$

Note: Calculated from $\Delta G^{\#} = -RT\ln k_2$ at $T = 40\,°C$.
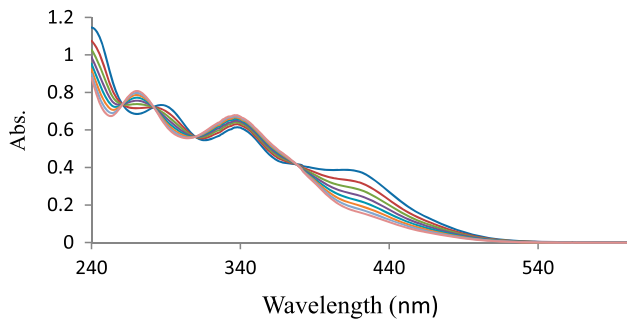

Figure 6. The absorption spectral changes with the isosbestic points during the reaction of $[UO_2(salpyr)(CH_3CN)]$, with an excess of PBu_3 at $10\,°C$ in acetonitrile.
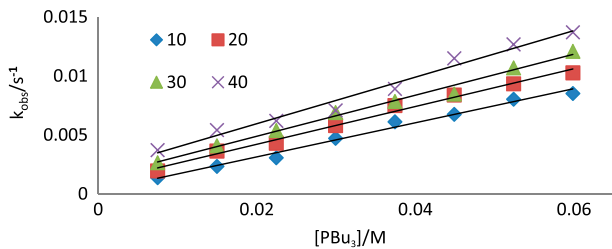

Figure 7. The plots of k_{obs} *vs.* $[PBu_3]$ for $[UO_2(3\text{-MeOsalpyr})(CH_3CN)]$ at different temperatures.

$$\Delta G^{\#} = -RT\ln k_2 \tag{7}$$

The k_2 values for the ligands showed high span, suggesting the dependence of the rate constant on the nature of the complex. The low $\Delta H^{\#}$ values and the large negative $\Delta S^{\#}$ values were compatible with an associative (A) mechanism. For studying the effect of substituents, we compared three complexes – 5-Br, 5-Cl, and 5-MeO so that the position of the group was the same but complexes differ in electronic properties; the obtained trend showed that k_2 for $[UO_2(5\text{-MeOsalpyr})(CH_3CN)]$ was the smallest because of the
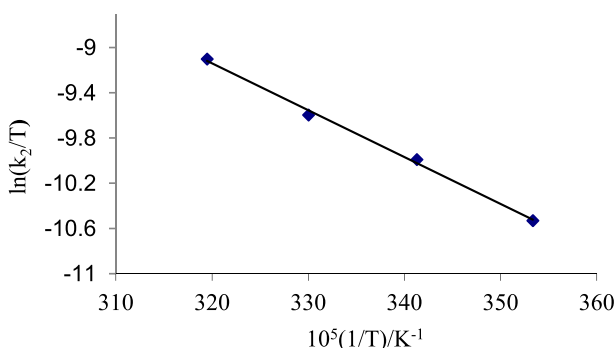
Figure 8. Eyring plot for the reaction of [UO$_2$(salpyr)(CH$_3$CN)] with excess PBu$_3$ in acetonitrile.

electron releasing group on the aromatic ring, while [UO$_2$(5-Clsalpyr)(CH$_3$CN)] showed the highest k_2 because of the electron withdrawing group. Existence of the chloro made the Schiff base complexes better acceptors. In [UO$_2$(5-Brsalpyr)(CH$_3$CN)], there was again an electron withdrawing group that was not very different from Cl and k_2 values confirmed this.

Then three other complexes – 3-MeO, 4-MeO, and 5-MeO were compared, but in this case the positions of the substituent differed. Methoxy is an electron releasing group, but this effect becomes strongest when methoxy was located para- to the oxygen of the phenyl ring. Thus k_2 values for 5-MeO were smaller than 4-MeO. When MeO was located in the ortho- position (3-MeO), the steric hindrance became more important than the electronic effect. According to the proposed mechanism, solvent in the 3-MeO complex was coordinated weakly, thus PBu$_3$ could interact with the complex faster than for 4-MeO and 5-MeO complexes.

Both electronic and steric effects took part during the exchange reaction, and the following trend was obtained: UO$_2$(5-Clsalpyr) > UO$_2$(5-Brsalpyr) > UO$_2$(3-MeOsalpyr) > UO$_2$(4-MeOsalpyr) > UO$_2$(salpyr) > UO$_2$(5-MeOsalpyr).

4. Conclusion

We synthesized uranyl asymmetric Schiff base complexes. By evaluating the X-ray structure of [UO$_2$(3-MeOsalpyr)(DMF)], one DMF coordinates weakly to uranium, while the other was not coordinated. Both DMF molecules were disordered. The presence of coordinated solvent was confirmed by thermal gravimetric studies. The kinetics and mechanism of solvent exchange reactions with tributylphosphine were investigated in acetonitrile. PBu$_3$ acted as a donor and replaced the weakly coordinated solvent. High span of k_2 as well as low $\Delta H^{\#}$ and large negative $\Delta S^{\#}$ suggested an associative (A) mechanism. Both electronic and steric effects were important for the rate of the exchange reaction. The trend of k_2 values showed that electron withdrawing groups like Cl, Br, and MeO in the meta position to the phenolic oxygen of the Schiff base accelerated the exchange reaction. On the other hand, electron releasing groups like MeO in the para-position to the phenolic oxygen of the Schiff base reduced the rate of the exchange reaction, because the uranium center was not very electron deficient. The steric effect was important in 3-MeO complex.

Z. Asadi et al.

Cyclic voltammetry was used to investigate the effect of substituents of ligands on reduction and oxidation of uranium $U^{(VI)} \leftrightarrow U^{(V)}$. Again, electron withdrawing groups accelerated the reduction of uranium.

Supplementary material

CCDC 926,790 contains the supplementary crystallographic data for this article. These data can be obtained free of charge from The Cambridge Crystallographic Data Center *via* www.ccdc.cam.ac.uk/data_request/cif. Supplemental data for this article can be accessed http://dx.doi.org/10.1080/00958972.2013.849343.

Acknowledgments

References

[1] K. Mizuoka, Y. Ikeda. *Inorg. Chem.*, **42**, 3396 (2003).
[2] M.F. Schettini, G. Wu, T.W. Hayton. *Inorg. Chem.*, **48**, 11799 (2009).
[3] K. Takao, M. Kato, S. Takao, A. Nagasawa, G. Bernhard, C. Hennig, Y. Ikeda. *Inorg. Chem.*, **49**, 2349 (2010).
[4] K. Takao, S. Tsushima, S. Takao, A.C. Scheinost, G. Bernhard, Y. Ikeda, C. Hennig. *Inorg. Chem.*, **48**, 9602 (2009).
[5] M.S. Bharara, K. Strawbridge, J.Z. Vilsek, T.H. Bray, A.E.V. Gorden. *Inorg. Chem.*, **46**, 8309 (2007).
[6] K. Takao, Y. Ikeda. *Inorg. Chem.*, **46**, 1550 (2007).
[7] K. Mizuoka, S. Tsushima, M. Hasegawa, T. Hoshi, Y. Ikeda. *Inorg. Chem.*, **44**, 6211 (2005).
[8] K. Mizuoka, S.Y. Kim, M. Hasegawa, T. Hoshi, G. Uchiyama, Y. Ikeda. *Inorg. Chem.*, **42**, 1031 (2003).
[9] K. Mizuoka, Y. Ikeda. *Inorg. Chem.*, **42**, 3396 (2003).
[10] J.D. Evans, P.C. Junk, M.K. Smith. *Polyhedron*, **21**, 2421 (2002).
[11] M. Asadi, Z. Asadi. *Int. J. Chem. Kinet.*, **39**, 137 (2007).
[12] M. Asadi, Z. Asadi, F. Mosalanezhad. *Int. J. Chem. Kinet.*, **42**, 499 (2010).
[13] Z. Asadi. *Int. J. Chem. Kinet.*, **43**, 247 (2011).
[14] M. Asadi, Z. Asadi, F. Mosalanezhad. *J. Iranian Chem. Soc.*, **8**, 794 (2011).
[15] V. Petricek, M. Dusek, L. Palatinus. *JANA 2006. Structure Determination Software Programs.*, Institute of Physics, Praha, Czech Republic (2008).
[16] N.S. Biradar, G.V. Karajagi, T.M. Aminabhavi, W.E. Rudzinski. *Inorg. Chim. Acta*, **82**, 211 (1984).
[17] L. Palatinus, G. Chapuis. *J. Appl. Cryst.*, **40**, 786 (2007).
[18] M. Asadi, Z. Asadi, S. Torabi, N. Lotfi. *Spectrochim. Acta (A)*, **94**, 372 (2012).
[19] M.A. Mokhles. *J. Chin. Chem. Soc.*, **48**, 153 (2001).
[20] M. Asadi, A.H. Sarvestani. *Can. J. Chem.*, **79**, 1360 (2001).
[21] M. Asadi, A.H. Sarvestani. *J. Chem. Research(s)*, 520 (2002).
[22] Z. Cimerman, N. Galešić, B. Bosner. *J. Mol. Struct.*, **274**, 131 (1992).
[23] V. Van axel Castelli, R. Cascciapagalia, G. Chiosos, C.J.M.F. van Veggel, L. Mandolini, D.N. Reinhoudt. *Inorg. Chem.*, **246**, 181 (1996).
[24] M.H. Koksal, M.K. Sener, S. Serin. *Transition Met. Chem.*, **24**, 414 (1999).